

SIMULATION OF TEXTURE DEVELOPMENT DURING DEFORMATION OF QUARTZITE

K. KUNZE, A. FRISCHBUTTER
Academy of Sciences, G.D.R.
Central Institute for Physics of the Earth
Telegraphenberg A51
POTSDAM, 1561
Germany

S. MATTHIES
Academy of Sciences, G.D.R.
Central Institute for Nuclear Research Rossendorf
PF 19
DRESDEN, 8051
Germany

INTRODUCTION

Numerical simulations of texture development based on the TAYLOR-BISHOP-HILL-theory have successfully been applied to deformation processes of metals, but also of quartz and other minerals¹⁻³. There has been found some important correspondence between simulated textures and observed c-axis patterns of naturally deformed quartzites^{4,5}. Less attention has been drawn to comparisons of the complete texture information given by the ODF. A number of quartz-ODF's has already been obtained by neutron or x-ray diffraction⁶⁻⁸, which should be compared with simulated textures.

In the paper a statistical approach to the flow field method⁹ directly realized in the orientation space has been adapted to quartz. It is based on a successful application of this concept to transformation and deformation texture development of f.c.c. metals^{10,11}. The results of TAYLOR simulations of two different model quartzites will be presented, obtained within the full constraint and two relaxed constraint models. The TAYLOR factor distribution and geometric hardening will be discussed.

THE METHOD

The orientation space is discretized by nonoverlapping spacefilling cells C_n ($n=1, N$) centred at g_n with volumes V_n . The ODF possesses a constant value f_n within each cell and is normalized according to

$$8\pi^2 = \sum_{n=1}^N V_n = \sum_{n=1}^N f_n V_n \quad (1)$$

Then the texture development after an elementary process step Δe is given by so-called "transition probabilities" $v_{mn}(e, \Delta e)$

$$f_m(e + \Delta e) = \sum_{n=1}^N f_n(e) v_{mn}(e, \Delta e) \quad (2)$$

with the normalization relations

$$V_n = \sum_{m=1}^N V_m v_{mn}. \quad (3)$$

If the investigated process can be separated into a number of equivalent steps Δe , which do not depend on the history e , then the weighting factors $v_{mn}(\Delta e)$ must be calculated only once. With the stored coefficients $v_{mn}(\Delta e)$ the development of any initial orientation distribution can easily be traced within a minimum computer time.

The orientation changes of transformation processes are usually large compared with the cell dimensions (5 degrees). Only the cell addresses k_n^j of the final orientations $g_n^j \in C(k_n^j)$ ($j=1, J_n$) for each initial orientation g_n will be determined. Then the transition factors read as follows

$$v_{mn} = V_n / V_m \sum_{j=1}^{J_n} w_n^j \delta_{m, k_n^j}, \quad \sum_{j=1}^{J_n} w_n^j = 1. \quad (4)$$

The weights w_n^j may take into account a variant selection.

Finite deformations are usually splitted into small steps, which cause only small orientation changes (comparable with the cell dimensions). As a rule the orientation density of an initial cell will only be transferred into the nearest neighbouring cells. To get the relative portions the initial cell is shifted by the orientation change Δg . The volume parts of the shifted cell, which overlap with the fixed cell grid, give the corresponding weight factors w_n^j . Eq. (4) remains true, where k_n^j are now the addresses of the overlapped cells.

The orientation changes Δg were obtained by the rigid-plastic TBH-theory for full constraint (FC) and relaxed constraint (RC) models. The required work minimization does not necessarily lead to an unique optimal solution of active glide system combinations. Such multiple solutions occupy the volume of polyhedrons in the configuration space. However, an infinite number of solutions can hardly be taken into account. A randomly selected solution or the mean of all corners of the polyhedron has commonly been used. To represent the whole polyhedron a set of discrete points is selected. It consists of the mean of the corners and some points situated on the lines from the centre to the corners at a distance reduced by a factor 2/3. All selected solutions are then considered in eq. (4).

The procedure directly provides the TAYLOR factor distribution $M(g_n)$. The relative equivalent stress for each step is obtained by the average

$$\bar{M}(e) = \sum_{n=1}^N M(g_n) V_n f_n(e) \quad (5)$$

The final ODF's have been smoothed substituting the discrete cell intensities by corresponding GAUSS-shaped standard functions at g_n with halfwidth $b=7.5^\circ$ within a harmonic series expansion up to $L=22$.

RESULTS

Two model quartzites have been investigated with glide systems and critical resolved shear stresses (crss) proposed earlier¹² (table 1). The low temperature set (LT) is characterized by easy {basal}<a> slip, whereas in the high temperature configuration (HT) easy {prism}<a> slip is additionally allowed. To satisfy the Von Mises criterion hard {rhom}<c+a> systems are added in both cases. Simulations have been performed for both

Table 1 Relative crss for slip systems of the models.

slip system	LT model	HT model
(0001)[21̄1̄0] {basal}<a>	1.0	1.0
(101̄0)[1̄21̄0] {prism}<a>	-	0.4
(101̄1)[1̄21̄0] {rhom}<a>	3.05	-
(011̄1)[21̄1̄0]	3.0	-
(101̄1)[1̄1̄23] {rhom}<a+c>	5.05	3.05
(011̄1)[1̄1̄23]	5.0	3.0

combinations in pure shear (PU), axialsymmetrical elongation (EL) and flattening (FL) within the FC model and in pure shear geometry within the lath and the pancake RC models for long (LG) or flat (FG) grains, respectively. The extension axis lies always N-S (Y_A -axis), the shortening axis E-W (X_A -axis) and the intermediate strain axis in pure shear is vertical (Z_A -axis). All runs started with an isotropic initial ODF $f(g)=1$.

The calculated stress-strain-curves for the FC model (fig. 1) completely coincide with those obtained by the single grain method¹². The LT quartzite becomes softer in flattening with increasing strain, whereas the HT quartzite becomes softer in elongation. All pure shear simulations show geometric hardening except the first deformation steps in the RC models where softening occurs. Each relaxation leads to a considerable decrease in the absolute average TAYLOR factor.

The distributions of the TAYLOR factor $M(g)$ and the resulting orientation density $f(g)$ are shown in spherical representations of σ -sections¹³

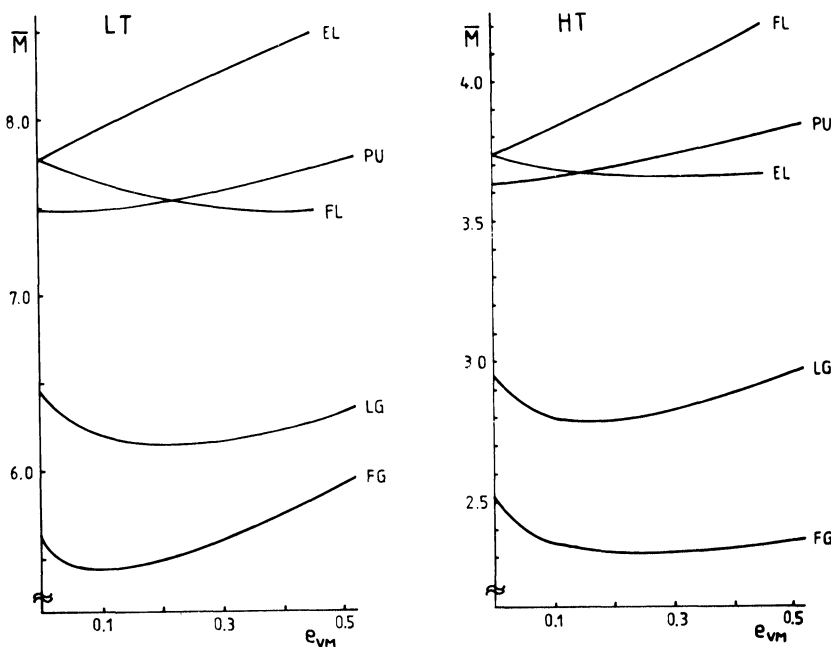


Figure 1 Average TAYLOR factor (relative equivalent stress) versus Von Mises equivalent strain for LT and HT quartzite in elongation (EL), flattening (FL), pure shear: FC (PU), RC-long grains (LG), RC-flat grains (FG)

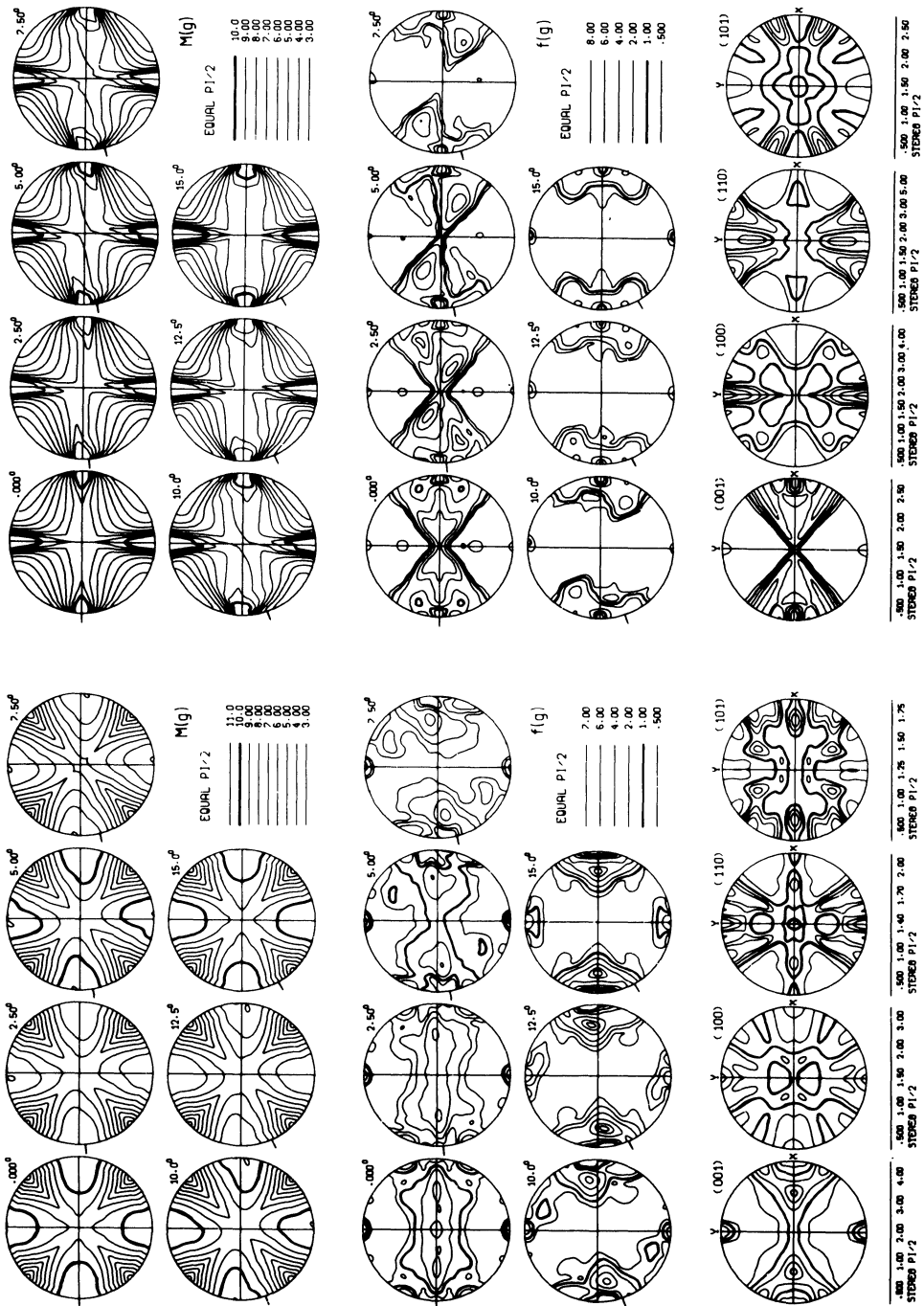


Figure 3 TAYLOR factor distribution $M(g)$, ODF $f(g)$ and pole figures for LT quartzite in pure shear. FC model (a), RC model - flat grains (b).

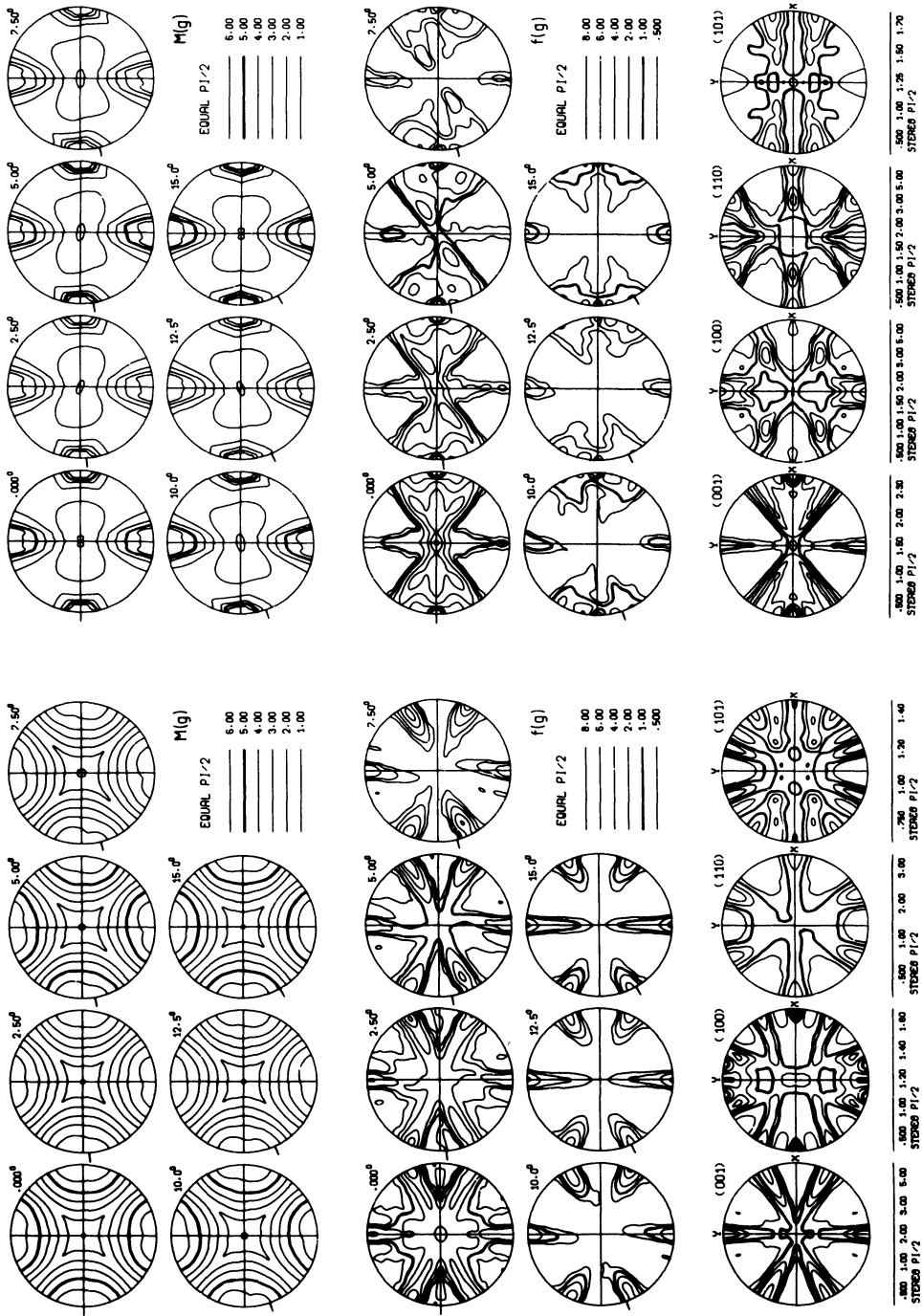


Figure 4 TAYLOR factor distribution $M(g)$, ODF $f(g)$ and pole figures for HT quartzite in pure shear. FC model (a), RC model - flat grains (b).

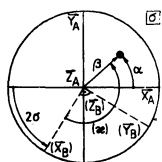


Figure 4 Definition of the angles α and β in a σ -section. In brackets inverse representation by $\alpha\beta = \pi - \gamma$ and β .

(fig. 2,3). Within every section of constant $\sigma = (\alpha + \gamma)/2$ an orientation $g = \{\alpha, \beta, \gamma\}$ (α, β, γ - ROE angles) is given by α and β , the spherical angles of the c-axis (Z_B) direction related to the sample system K_A (fig. 4). The sum of all σ -sections directly gives the c-axis pole figure.

The TAYLOR factor varies with g remarkably. Orientations with c-axes parallel to the extension or the shortening axis possess a maximum TAYLOR factor. The minimum lies between both axes for the LT quartzite, but parallel to the medium strain axis for the HT quartzite. The extreme values do not considerably differ for the FC and RC models. Only the gradients of the TAYLOR factor distributions become somewhat sharper in the RC models. The TAYLOR factors are nearly independent on σ (or γ), i.e. they are almost axialsymmetrical with regard to rotations about the c-axis.

Because of the required homogeneous deformation in the FC model grains are not allowed to rotate into soft orientations. Relatively hard orientations are preferred. The c-axis patterns show the known structure - combined two girdles for LT quartzite and crossed girdles for HT quartzite.

Relaxation of some shear components admits heterogeneous deformation. Grains tend towards softer orientations. However, the freedom opened by the relaxed components is not sufficient that only the softest orientations would be occupied. In HT quartzite a maximum by $g = \{0, 0, 0\}$ (c-axis in the medium strain axis) arises. This soft orientation often observed in naturally deformed quartzites has never been produced by FC models.

Strain heterogeneities seem to be a substantial feature of deformation of quartzite and even more of quartz-bearing polyphase rocks. The investigations support recent conclusions from viscoplastic self-consistent calculations¹⁴, where strain incompatibility has more generally been considered than in models with relaxation of only certain deformation components.

REFERENCES

1. G.S.Lister, M.S.Paterson, B.E.Hobbs, *Tectonophysics*, 45, 107 (1978)
2. G.S.Lister, B.E.Hobbs, *J.Struct.Geol.*, 2, 355 (1980)
3. H.-R.Wenk (Ed.), *Preferred Orientation in Deformed Metals and Rocks: An Introduction to Modern Texture Analysis* (Academic Press, Orlando Fla. 1985)
4. G.P.Price, cf. ref.3, p.385
5. A.Ord, in: J.S.Kallend, G.Gottstein (Ed.), *Proc. ICOTOM 8* (Santa Fe, 1988) p.765
6. H.J.Bunge, H.-R.Wenk, *Tectonophysics*, 40, 257 (1977)
7. S.M.Schmid, M.Casey, J.Starkey, *Tectonophysics*, 78, 101 (1981)
8. V.Damm, K.Feldmann, A.Frischbutter, W.Kleinsteuber, K.Walther, *Textures and Microstructures*, 12, 15 (1990)
9. H.J.Bunge, C.Esling, E.Dahlem, H.Klein, *Textures and Microstructures*, 6, 181 (1986)
10. T.Steinkopff, S.Matthies, cf. ref.5, p.49
11. T.Steinkopff, thesis, Rossendorf (1989)
12. T.Takeshita, H.-R.Wenk, *Tectonophysics*, 149, 345 (1988)
13. S.Matthies, K.Helming, K.Kunze, *phys.stat.sol.(b)*, 157, 71 (1990); 489 (1990)
14. H.-R.Wenk, G.Canova, A.Molinari, U.F.Kocks, *J.Geophys.Res.* (1990)